Polymer Journal (2019) 51:1147–1161
https://doi.org/10.1038/s41428-019-0228-x

ORIGINAL ARTICLE

Adamantane-containing poly(dialkyl fumarate)s with rigid chain structures

Nagisa Tsuji[1] · Yasuhito Suzuki[1] · Akikazu Matsumoto[1]

Received: 15 April 2019 / Revised: 4 June 2019 / Accepted: 10 June 2019 / Published online: 8 July 2019

Abstract

Four dialkyl fumarates containing bulky adamantyl ester groups, i.e., di(1-adamantyl) fumarate (**1**), bis(3,5-dimethyl-1-adamantyl) fumarate (**2**), 1-adamantyl isopropyl fumarate (**3**), and 3,5-dimethyl-1-adamantyl isopropyl fumarate (**4**), were polymerized to obtain poly(dialkyl fumarate)s (PDRFs) with rigid chain structures. We carried out the conventional radical polymerization of these adamantane-containing DRFs in the presence of a radical initiator either in toluene or in bulk at 80 or 60 °C. Reversible addition-fragmentation chain transfer (RAFT) polymerization was also performed using 1,1′-(1,2-ethanediyl) bis[2-[[(dodecylthio)thioxymethyl]thio]-2-methylpropionate] and 2,2,2-trifluoroethyl 2-[[(dodecylthio)thioxymethyl]thio]-2-methylpropionate as the chain transfer agents (CTAs). Triblock copolymers consisting of rigid and flexible segments were synthesized by the polymerization of 2-ethylhexyl acrylate, which was used as the second monomer, using the PDRFs as the macro-CTA containing trithiocarbonate groups at the chain ends. The excellent thermal stability of the adamantane-containing PDRFs was confirmed by thermogravimetric analysis in a nitrogen stream. The alignment of the rigid PDRF chains in the solid-state was revealed based on the appearance of a peak in the small angle regions of the X-ray diffraction profiles.

Introduction

The radical polymerization of dialkyl fumarates yields poly (dialkyl fumarate)s (PDRFs) [1–3] with rigid chain conformations [4–8]. PDRFs are high-temperature and transparent polymer materials that are useful for information and electronics applications, such as in coatings, disks, fibers, displays, electronic devices, solar cells, etc [9–12]. PDRFs do not contain a methylene spacer in their main chain in contrast to conventional vinyl polymers that contain a flexible methylene spacer in every repeating monomer unit. The rigidity of the PDRF chains was evaluated using an analysis of the viscosity of PDRFs and light scattering data of a dilute PDRF solution using worm-like chain models [13–17]. The alignment and anisotropic features of these PDRF chains and their resulting unique solid-state properties have also been reported in the literature [9, 10]. Recently, we reported the reversible addition-fragmentation chain transfer (RAFT) polymerization of diisopropyl fumarate (DiPF) and the synthesis of block copolymers consisting of a less-flexible poly(diisopropyl fumarate) (PDiPF) segment and a flexible polyacrylate segment [18–20].

Adamantane (tricyclo[3.3.1.1^{3,7}]decane) is a thermodynamically stable and highly symmetrical tricyclic hydrocarbon and consists of fused chair-form cyclohexane rings with the same structure as a diamond lattice [21]. The syntheses of many polymers containing an adamantyl moiety in their main or side chains have been reported in the literature [22–33] and exploit the unusual physical and chemical properties of adamantane, for example, its thermodynamic stability, high melting point, thermal and oxidation stabilities, low surface energy, volatility, high density, and hydrophobicity. Thirty years ago, Otsu et al. reported the superior thermal properties of various acrylic polymers containing adamantyl moieties in their side chains, for example, acrylates [34], methacrylates [34–36],

Supplementary information The online version of this article (https://doi.org/10.1038/s41428-019-0228-x) contains supplementary material, which is available to authorized users.

✉ Akikazu Matsumoto
matsumoto@chem.osakafu-u.ac.jp

[1] Department of Applied Chemistry, Graduate School of Engineering, Osaka Prefecture University, 1-1 Gakuen-cho, Naka-ku, Sakai, Osaka 599-8531, Japan

itaconates [37], fumarates [38], crotonates [6], and sorbates [39]. Later, Ishizone and coworkers reported the living anionic polymerization of adamantane-containing styrene and butadiene derivatives to synthesize functional polymers and block copolymers [40–47]. Several years ago, Nakano et al. reported the synthesis of sequence-controlled block copolymers comprising poly(1-adamantyl acrylate) (PAdA) and poly(*n*-butyl acrylate) sequences, which were used as the hard and soft segments, respectively, by organotellurium-mediated living radical polymerization (TERP) [48]. The thermal, optical, and mechanical properties of the adamantane-containing block copolymers were investigated in detail. More recently, the dynamic mechanical properties of random copolymers of DiPF containing 1-adamantyl acrylate (AdA) or bornyl acrylate repeating units were studied to determine the chain dynamics specific to a rigid poly(substituted methylene) structure [49, 50].

In this study, four types of adamantane-containing DRFs, i.e., di(1-adamantyl) fumarate (**1**), bis(3,5-dimethyl-1-adamantyl) fumarate (**2**), 1-adamantyl isopropyl fumarate (**3**), and 3,5-dimethyl-1-adamantyl isopropyl fumarate (**4**) were prepared (Fig. 1). A preliminary study by Matsumoto and Otsu previously reported the synthesis of these monomers using conventional radical polymerization [38], but a detailed study has not been carried out in the past thirty years to synthesize and characterize these adamantane-containing fumarate polymers. In this study, we polymerized these monomers in the presence of a radical initiator either in solution or in bulk to obtain thermally stable PDRFs. Furthermore, reversible addition-fragmentation chain transfer (RAFT) polymerization using 1,1′-(1,2-ethanediyl) bis[2-[[(dodecylthio)thioxymethyl] thio]-2-methylpropionate] (T2) and 2,2,2-trifluoroethyl 2-[[(dodecylthio)thioxymethyl]thio]-2-methylpropionate [51] (T1F) as the chain transfer agents (Fig. 1) was performed to produce block copolymers consisting of rigid PDRF and flexible poly(2-ethylhexyl acrylate) (P2EHA) segments. The alignment of the PDRF segments in the solid-state was investigated by X-ray diffraction.

Experimental methods

Materials

DiPF and 2-ethylhexyl acrylate (2EHA) were purchased from Tokyo Chemical Industry, Co., Ltd. (Tokyo, Japan) and distilled under a reduced pressure before use. Dimethyl 2,2′-azobisisobutyrate (MAIB) was purchased from Wako Pure Chemical Industries, Ltd. (Osaka, Japan) and recrystallized from *n*-hexane. 2,2′-Azobisisobutyronitrile (AIBN) was purchased from Nacalai Tesque, Ltd. (Kyoto, Japan) and used after recrystallization from methanol. Benzoyl peroxide (BPO, containing 25% water) was purchased from Nacalai Tesque, Ltd. (Kyoto, Japan) and used without further purification. 1-Adamantanol, *N*,*N*-dimethylaminopyridine (DMAP) and *N*,*N*'-dicyclohexylcarbodiimide (DCC) were purchased from Tokyo Chemical Industry, Co., Ltd. (Tokyo, Japan) and used without further purification. Maleic anhydride and sulfuric acid were purchased from Kishida Chemical Industry, Co., Ltd. (Tokyo, Japan) and used as received. 3,5-Dimethyl-1-adamantanol, piperidine, and 2-propanol were purchased from Wako Pure Chemical Industries, Ltd. (Osaka, Japan) and used without further purification. The solvents were purchased from Wako Pure Chemical Industries, Ltd. (Osaka, Japan) and used after distillation. T2 was synthesized according to a previously reported method [20].

Synthesis of 1

Three drops of concentrated sulfuric acid were added to maleic anhydride (0.983 g, 10 mmol) and 1-adamantanol (3.35 g, 22 mmol) in 50 mL of cyclohexane, and then, the mixture was refluxed for 4 h. After the reaction, the solution was washed twice with saturated aq. $NaHCO_3$ and then once with saturated aq. NaCl. After drying over sodium sulfate, the filtrate was concentrated under a reduced pressure, resulting in the precipitation of a white solid. The crude yield was 2.48 g (65%). The product was recrystallized from a mixture of ethanol and toluene (5/1 by

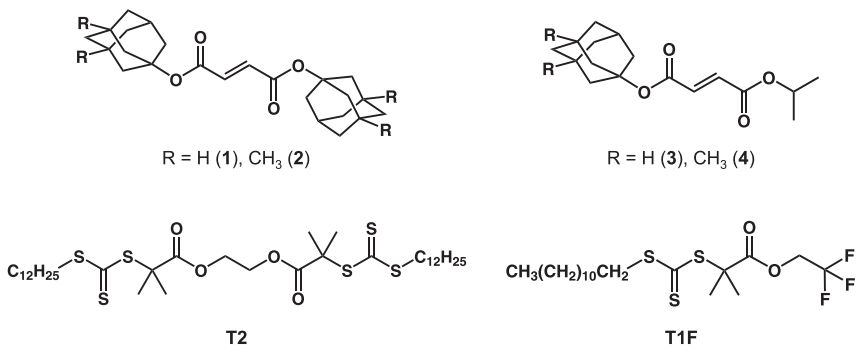

Fig. 1 Chemical structure of the DRFs and RAFT agents used in this study

volume) and then dried in vacuo at room temperature. The product included a small amount of the corresponding monoester but was used for the subsequent isomerization without further purification.

Di-1-adamantyl maleate

Yield 1.18 g, white solid, m.p. 103–110 °C (lit. 146 °C) [38]. ^{1}H NMR (400 MHz, $CDCl_3$) δ (ppm) 6.05 (s, CH = , 2 H), 2.17 (m, CH_2 and CH, 18 H), 1.75–1.63 (m, CH_2, 12 H).

Di-1-adamantyl maleate (1.00 g, 2.6 mmol) in 40 mL of cyclohexane was refluxed for 3.5 h in the presence of 0.25 mL of piperidine. After removing the solvent, a white solid was isolated. Silica gel chromatography was performed using a mobile phase containing hexane/ethyl acetate/chloroform = 85/5/10, by volume, and subsequent drying provided the corresponding fumarate **1**.

1: Yield 0.31 g (31%), m.p. 191.8 °C (lit. 192 °C) [38]. ^{1}H NMR (400 MHz, $CDCl_3$) δ (ppm) 6.65 (s, CH = CH, 2 H), 2.18 (s, CH, 6 H), 2.14 (m, CH_2, 12 H), 1.71–1.64 (m, CH_2, 12 H); ^{13}C NMR (100 MHz, $CDCl_3$) δ (ppm) 164.3 (C = O), 134.8 (C = C), 81.9 (OC), 41.4 and 36.3 (CH_2), 31.0 (CH).

Synthesis of 2

Bis(3,5-dimethyl-1-adamantyl) maleate was synthesized from maleic anhydride and 3,5-dimethyl-1-adamantanol according to a procedure similar to that used to synthesize **1**.

Bis(3,5-dimethyl-1-adamantyl) Maleate

Yield 2.9 g (66%), m.p. 64.5–65.5 °C (Lit. 86.0 °C) [38]. ^{1}H NMR (400 MHz, $CDCl_3$) δ (ppm): 6.03 (s, CH = CH, 2 H), 2.31–1.74 and 1.43–1.09 (m, CH and CH_2, 26 H), 0.88 (s, CH_3, 12 H).

2 was obtained by the isomerization of bis(3,5-dimethyl-1-adamantyl) maleate in the presence of piperidine and purified by silica gel chromatography using a mobile phase containing hexane/ethyl acetate/chloroform = 80/10/10, by volume.

2: Yield 0.99 g (37%), m.p. 70.2 °C (Lit. 70.0 °C) [38]. ^{1}H NMR (400 MHz, $CDCl_3$) δ (ppm) 6.62 (s, CH = CH, 2 H), 2.27–1.65 and 1.47–1.07 (m, CH and CH_2, 26 H), 0.88 (s, CH_3, 12 H). ^{13}C NMR (100 MHz, $CDCl_3$) δ (ppm) 164.3 (C = O), 134.8 (C = C), 83.2 (OC), 50.5, 47.2, 42.3, 39.8, 34.1, 31.2, and 30.0 (CH, CH_2, and CH_3).

Synthesis of 3 and 4

3 was synthesized according to the following procedures. Maleic anhydride (4.9 g, 0.05 mol) and 2-propanol (3.0 g, 0.05 mol) were refluxed in 130 mL of cyclohexane for 13 h in the absence of an acidic catalyst to synthesize isopropyl maleate monoester. The resulting solution was used for the subsequent reactions without isolating the product.

Isopropyl maleate monoester

^{1}H NMR (400 MHz, $CDCl_3$) δ (ppm) 6.465 (d, J = 12.8 Hz, CH = C<u>H</u>COOCH(CH_3)$_2$, 1 H), 6.335 (d, J = 12.8 Hz, CH = C<u>H</u>COOH, 1 H), 5.24–5.14 (m, CH, 1 H), 1.355 (d, J = 6.2 Hz, CH_3, 6 H).

To the abovementioned solution, 1-adamantanol (7.6 g, 0.05 mol) and ca. 0.5 mL of concentrated sulfuric acid were added, and then, the mixture was refluxed for 22 h. After the reaction, the solution was washed twice with saturated aq. $NaHCO_3$ and then once with saturated aq. NaCl. After drying over sodium sulfate, the filtrate was concentrated under a reduced pressure to produce a white paste. The product was a mixture of the diesters and monoesters of maleic acid. Repeated silica gel chromatography using a mobile phase containing hexane/diethyl ether/acetone = 70/10/20, by volume, yielded 1-adamantyl isopropyl maleate as the main product, which was a colorless liquid.

1-Adamantyl isopropyl maleate

Yield 1.8 g (12%). ^{1}H NMR (400 MHz, $CDCl_3$) δ (ppm) 6.145 (d, J = 10.7 Hz, CH = C<u>H</u>COOCH(CH_3)$_2$, 1 H), 6.095 (d, J = 10.7 Hz, CH = C<u>H</u>COO$C_{10}H_{15}$, 1 H), 5.18–5.08 (m, CH, 1 H), 2.17 and 1.71–1.63 (m, $C_{10}H_{15}$, 15 H), 1.29 (d, J = 6.4 Hz, CH_3, 6 H).

1-Adamantyl isopropyl maleate (1.8 g) in 40 mL of toluene was refluxed for 2 h in the presence of 0.25 mL of piperidine. After removing the solvent, a yellow viscous liquid was isolated. After the product was diluted with chloroform, it was washed twice with saturated aq. $NaHCO_3$ and once with saturated aq. NaCl and then dried over sodium sulfate. After the filtrate was concentrated under a reduced pressure, silica gel chromatography using a mobile phase containing hexane/diethyl ether/acetone = 85/5/10, by volume, yielded **3**, which was a colorless liquid. The yield was 1.51 g (84%). **4** was synthesized according to a similar procedure.

3: ^{1}H NMR (400 MHz, $CDCl_3$) δ (ppm) 6.755 (d, J = 12.0 Hz, CH = C<u>H</u>COOCH(CH_3)$_2$, 1 H), 6.705 (d, J = 12.0 Hz, CH = CHCOO$C_{10}H_{15}$, 1 H), 5.15–5.06 (m, CH, 1 H), 2.19 and 1.71–1.64 (m, $C_{10}H_{15}$, 16 H), 1.285 (d, J = 6.4 Hz, CH_3, 6 H). ^{13}C NMR (100 MHz, $CDCl_3$) δ (ppm) 164.9 and 164.0 (C = O), 135.6 and 133.2 (C = C), 82.0 (OC), 68.8 (OCH), 41.3 and 36.2 (CH_2), 30.9 (CH), 21.8 (CH_3).

4: ^{1}H NMR (400 MHz, $CDCl_3$) δ (ppm) 6.750 (d, J = 12.0 Hz, CH = CHCOOCH(CH_3)$_2$, 1 H), 6.703 (d, J = 12.0 Hz, CH = CHCOO$C_{12}H_{19}$, 1 H), 5.14–5.05 (m, CH for

$COOCH(CH_3)$, 1 H), 2.18–1.60 and 1.31–1.23 (m, CH and CH_2 for $COOC_{10}H_{13}(CH_3)_2$, 13 H), 0.88 (s, CH_3 for $COOC_{10}H_{13}(CH_3)_2$, 6 H). ^{13}C NMR (100 MHz, $CDCl_3$) δ (ppm) 164.9 and 164.1 (C = O), 135.6 and 133.2 (C = C), 82.0 (OC), 68.9 (OCH), 50.5, 47.2, 42.6, 41.3, 39.8, 36.2, 34.1, 31.2, 31.0, 30.0, and 21.9 (CH, CH_2, and CH_3).

Synthesis of T1F

T1F was synthesized as follows. To a mixture of 2-[[(dodecylthio)thioxymethyl]thio]-2-methylpropanoic acid (1.10 g, 3.0 mmol), 2,2,2-trifluoroethanol (0.908 g, 9.1 mmol), and DMAP (36.7 mg, 0.30 mmol) in 20 mL of chloroform (super dehydrated grade), DCC (0.65 g, 3.2 mmol) in 5 mL of chloroform was added dropwise with stirring at 0 °C, and the mixture was further stirred at 0 °C for 1 h and then stirred at room temperature for 72 h. The filtrate was concentrated and purified by column chromatography (silica gel, hexane/chloroform = 1/1, by volume).

Yellow liquid. Yield 0.50 g (38%). ^1H NMR (400 MHz, $CDCl_3$) δ (ppm) 4.46 (q, $J = 8.5$ Hz, CF_3CH_2, 2 H), 3.27 (t, $J = 7.4$ Hz, SCH_2, 2 H), 1.72 (s, CH_3, 6 H), 1.68–1.26 (m, $(CH_2)_{10}$, 20 H), 0.88 (t, $J = 6.6$ Hz, $CH_2\underline{CH}_3$, 3 H). ^{13}C NMR (100 MHz, $CDCl_3$) δ (ppm) 221.5, 172.0, 123.0 (q, $J = 276$ Hz), 61.7 (q, $J = 36$ Hz), 55.6, 37.2, 32.1, 29.77, 29.76, 29.68, 29.56, 29.48, 29.0, 27.9, 25.3, 22.8, and 14.3.

Conventional radical polymerization

A monomer and a radical initiator were placed in a glass tube in the presence or absence of a solvent. After freeze–thaw cycles (three times) were performed to remove any oxygen, the solution was heated at a specific temperature. After polymerization, the solution was diluted with a small amount of chloroform or toluene and then poured into a large amount of methanol to precipitate the polymers. Hot ethanol was used as the precipitant for the polymerization of **1**. The polymer yield was determined based on the weight of the isolated polymers. The isolated polymers were purified by reprecipitation and used for the SEC and NMR measurements.

RAFT polymerization

A monomer, radical initiator, and CTA were placed in a glass tube. After freeze–thaw cycles (three times) were performed to remove any oxygen, the solution was heated at 80 or 60 °C. An aliquot of the polymerization solution was analyzed by ^1H NMR spectroscopy to determine the conversion of the monomers. After polymerization, the solution was diluted with a small amount of chloroform and then poured into a large amount of methanol to precipitate the polymers. The polymer yield was determined based on the weight of the isolated polymers. The isolated polymers were purified by reprecipitation and used for the SEC and NMR measurements. The theoretical number-average molecular weight ($M_{n,cacld}$) was calculated according to Eq. 1.

$$M_{n,calcd} = \left(MW_{monomer} \times [monomer]_0 \times \% \text{ conversion} \times 0.01\right)/[CTA]_0 + MW_{CTA} \quad (1)$$

where $MW_{monomer}$ and MW_{CTA} are the molecular weights of the monomers and CTAs, respectively, and $[monomer]_0$ and $[CTA]_0$ are the initial concentrations of the monomers and CTAs, respectively.

Synthesis of block copolymers

Triblock copolymers of PDRF and P2EHA [or poly(methyl acrylate) (PMA)] were synthesized according to a procedure similar to that reported in a previous study [20]. The PDRFs prepared by RAFT polymerization using T2 as the CTA were used as the macro-CTA. An acrylate monomer, a radical initiator, and the macro-CTA were placed in a glass tube. After freeze–thaw cycles (three times) were performed to remove any oxygen, the solution was heated at 60 °C. An aliquot of the polymerization solution was analyzed by ^1H NMR spectroscopy to determine the conversion of the acrylate monomers. After polymerization, the solution was diluted with a small amount of chloroform and then poured into a large amount of methanol to precipitate the polymers. The polymer yield was determined based on the weight of the isolated polymers. The isolated polymers were purified by reprecipitation and used for the SEC and NMR measurements. The DRF content in the copolymers were estimated by the results of the NMR spectroscopy and SEC analysis.

Measurements

The ^1H NMR spectra were recorded using JEOL ECS-400 and ECX-400 spectrometers with chloroform-*d* at room temperature. The number average and weight average molecular weights (M_n and M_w) were determined by size exclusion chromatography (SEC) with tetrahydrofuran as the eluent at 40 °C and using a system consisting of a JASCO PU-2080-Plus pump, a JASCO DG-2080-53 degasser, a Chromato Science CS-300C thermostat chamber, Tosoh TSK gels GMHHR-N and GMHHR-H columns, a JASCO RI-2031-Plus RI detector, and a JASCO UV-2031-Plus UV detector (300 nm). The molecular weights were calibrated using polystyrene standards (Tosoh Corporation, Ltd., Japan) [19]. The thermogravimetric (TG) analysis was carried out using a Shimadzu DTG-60 analyzer, and measurements were obtained under a nitrogen stream at a heating rate of 10 °C/min. The onset temperature

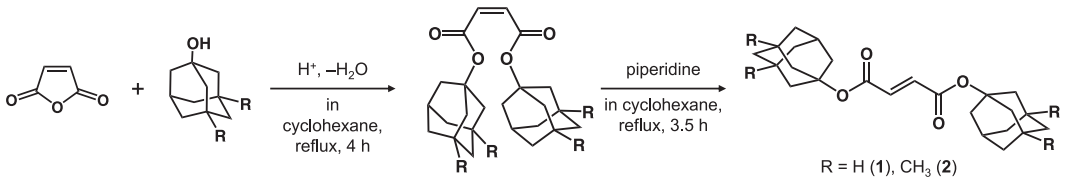

Scheme 1 Synthesis of the symmetric DRFs containing adamantyl esters **1** and **2**

of decomposition (T_{d5}) was determined to be the temperature at which 5% weight loss was observed. The maximum decomposition temperature (T_{max}) was determined by taking the derivative of a peak in the TG curves. The synchrotron radiation experiments were performed at the BL40B2 of the SPring-8 beamline (Hyogo, Japan). X-rays with a wavelength of 1.0 Å were exposed for 1 s at room temperature. The scattering patterns were recorded using a 1032 × 1032 pixel flat panel detector (Hamamatsu Photonics, C9278DK, pixel size = 50 µm × 50 µm) with a camera distance of 85.37 mm. The UV-vis spectra were recorded using a UV-2450 spectrophotometer (Shimadzu, Kyoto, Japan) to evaluate the transmittance of the polymer films, which were prepared by casting and drying a 5 wt% polymer solution in chloroform on a quartz plate. The thickness of the polymer films was 55–65 µm. The refractive indices (n_D, n_D, n_F, and n_C) were measured at wavelengths of 486, 546, 589, and 656 nm, respectively, using an Abbe-type refractometer (Atago DRM2, 1-bromonaphthalene, a halogen lamp, Tokyo, Japan), and the polymer films (thickness 100–120 µm) were prepared by casting 10 wt% chloroform solutions. The Abbe number (ν_D) was calculated using the following equation.

$$\nu_D = (n_D - 1)/(n_F - n_C) \quad (2)$$

The calculated refractive index values were fitted with the experimental results using the Cauchy equation (Eq. 3) as the two-parameter (n_∞ and D) analysis method [52].

$$n_\lambda = n_\infty + D/\lambda^2 \quad (3)$$

where λ is the wavelength, n_∞ is the refractive index at an infinite wavelength, n_λ is the refractive index at wavelength λ, and D is a constant.

Results and discussion

Synthesis of Adamantane-containing DRF

1 and **2** were synthesized from maleic anhydride and 1-adamantanol or 3,5-dimethyl-1-adamantanol, respectively, in the presence of an acidic catalyst in cyclohexane after refluxing for 4 h, and then, the resulting maleates were isomerized to the corresponding fumarates in the presence of piperidine in the same solvent while refluxing for 3.5 h (Scheme 1). Silica gel column chromatography yielded **1** and **2**, which presented as white crystals, with 31–37% yields. The melting points were 191.8 and 70.2 °C for **1** and **2**, respectively. The ^{1}H NMR spectra of **1** and **2** are shown in Fig. 2.

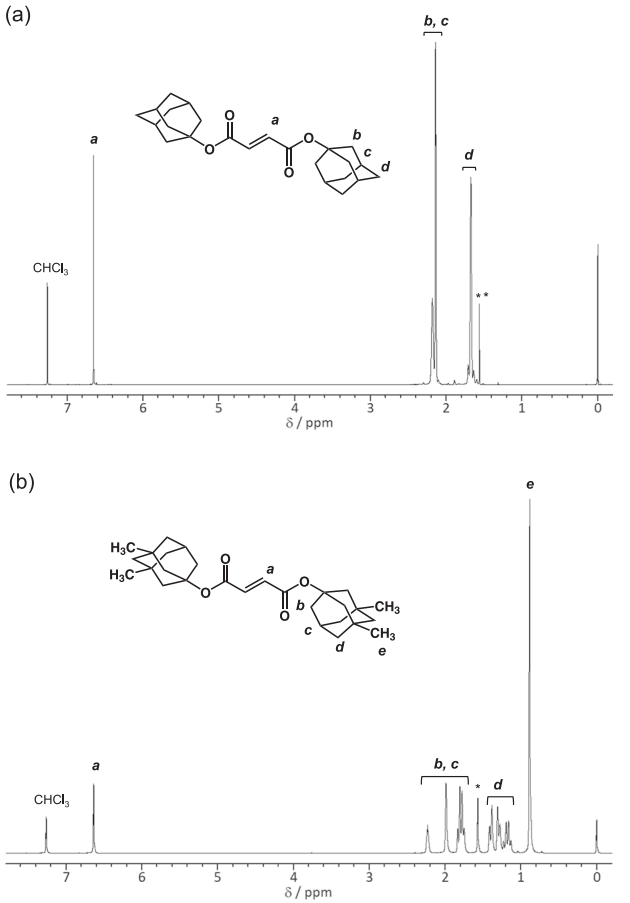

Fig. 2 ^{1}H NMR spectra of **a 1** and **b 2** in $CDCl_3$. Asterisk indicates the peak attributed to H_2O

The asymmetric fumarates were synthesized according to the reactions shown in Scheme 2. The equimolar amounts of maleic anhydride and 2-propanol were reacted in cyclohexane while refluxing in the absence of an acid for 13 h. Then, 1-adamantanol and a small amount of sulfuric acid were added to the solution, and the reaction

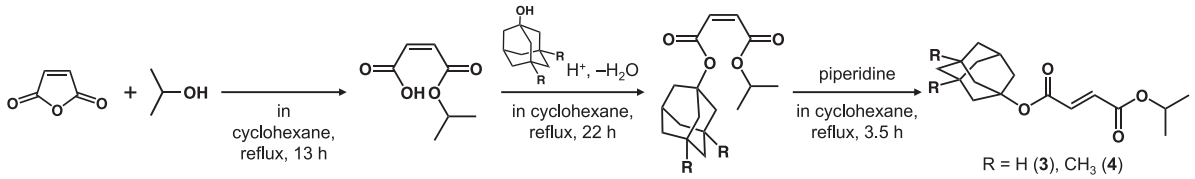

Scheme 2 Synthesis of the asymmetric DRFs containing adamantyl esters **3** and **4**

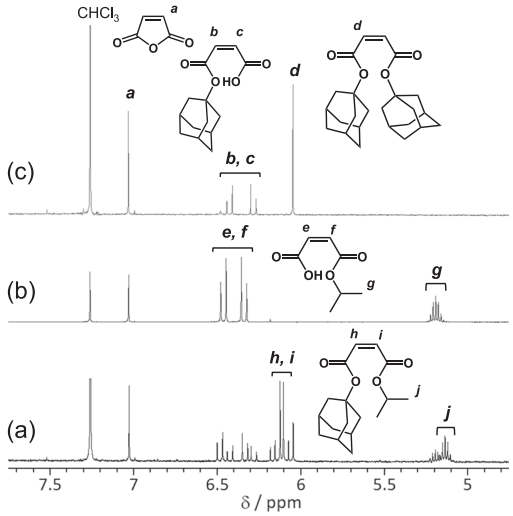

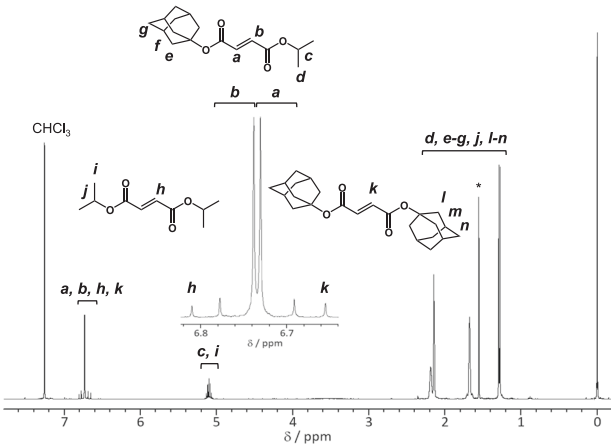

Fig. 4 ^{1}H NMR spectrum of **3** in $CDCl_3$. Asterisk indicates the peak attributed to H_2O

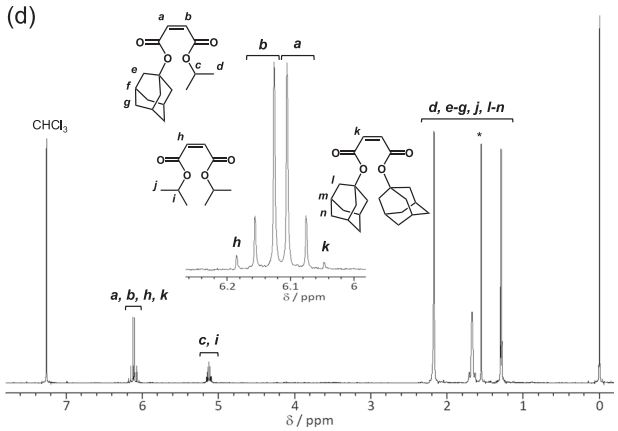

Fig. 3 ^{1}H NMR spectra of **a** a reaction mixture containing isopropyl maleate and 1-adamantanol in the presence of an acid, refluxed in cyclohexane for 22 h, **b** a reaction mixture containing maleic anhydride and isopropanol in the absence of an acid, refluxed in cyclohexane for 19 7h, **c** a reaction mixture containing maleic anhydride and isopropanol in the absence of an acid, refluxed in cyclohexane for 10 h, and **d** 1-adamantyl isopropyl maleate isolated after purification by column chromatography and containing a small amount of diisopropyl maleate and di-1-adamantyl maleate. Measured in $CDCl_3$

mixture was refluxed for 22 h. After the evaporation of the solvent, the ^{1}H NMR spectrum of the crude product indicated the presence of three types of the maleic diesters in a product mixture; i.e., 1-adamantyl isopropyl maleate was the main product and diisopropyl maleate and di-1-adamantyl maleate were the side products, as shown in Fig. 3a. The symmetric diesters were produced by transesterification during reflux in the presence of an acid. In addition to the diesters, the maleic acid monoesters as well as an unreacted maleic anhydride were also detected. The peaks characteristic of the isopropyl monoester and the 1-adamantyl monoester of maleic acid [see the spectra in Fig. 3b, c] are included in the ^{1}H NMR spectrum. The unreacted maleic anhydride and the monoesters of maleic acid were readily removed from the reaction mixture by washing with saturated aq. $NaHCO_3$. In contrast, the isolation of 1-adamantyl isopropyl maleate, which is the asymmetric fumaric diester, from the mixture of the three diesters was achieved by repeated silica gel column chromatography (*n*-hexane/ethyl acetate/chloroform = 7/1/2). We isolated 1-adamantyl isopropyl maleate as a colorless liquid with a purity of 92%. The isolated yield was 12%.

The isomerization of 1-adamantyl isopropyl maleate to the corresponding fumarate, i.e., **3**, was carried out in cyclohexane while refluxing in the presence of piperidine (Scheme 2). Silica gel column chromatography yielded **3**, which presented as a colorless liquid, with a high purity (>96%) and 84% yield, which was calculated based on the use of 1-adamantyl isopropyl maleate (Fig. 4). Similarly, **4**

was synthesized and isolated as a colorless liquid. The NMR spectral data of the DRFs used in this study are summarized in Table 1.

Conventional radical polymerization

The adamantane-containing DRFs were polymerized in the presence of a radical initiator (Scheme 3) under the polymerization conditions shown in Table 2. **1** had a high melting point and exhibited a low solubility in organic solvents. The solution polymerization of **1** yielded an oligomer with an M_n less than 10^4. The separation of the resulting **P1** from the remaining monomer **1** was achieved after repeated precipitation using chloroform as the solvent and hot ethanol as the precipitant.

The introduction of methyl substituents to the 3- and 5-positions of the adamantyl group led to a drastic decrease in the melting point and the improved solubility of the monomer. The bulk polymerization of **2** with BPO at 80 °C yielded a polymer with a 26% yield. The obtained polymer **P2** was supposed to have a high molecular weight, because the viscosity increased during polymerization. In fact, the chloroform solution of **P2** had a high viscosity, but **P2** was insoluble in THF. Therefore, the molecular weight was not determined by the SEC measurement in this study. The solution polymerization provided a soluble polymer with an M_n less than 10^4.

The asymmetric DRFs, i.e., **3** and **4**, yielded high molecular weight polymers in high yields during bulk polymerization in the presence of MAIB at 60 °C (Scheme 4). The solution polymerization again yielded polymers with a low M_n. Previous studied reported that polymerization at a high monomer concentration was required to produce PDRFs with a high molecular weight and a high yield [3, 4]. The monomers **3** and **4** were liquids at room temperature, so they are suitable for high polymerization under bulk conditions. The produced polymers **P3** and **P4** were soluble in toluene, chloroform, and THF. The ^{1}H NMR spectra of the isolated polymers are shown in Fig. 5. The peaks characteristic to the repeating units, i.e., the methyl, methylene, and methine hydrogens of the 1-adamantyl and 3,5-dimethyl-1-adamantyl ester groups, were observed as the broad peaks in the range of 0.7–2.5 ppm. For **P3** and **P4**, the methyl and methine hydrogens of the isopropyl group were also detected ca. 1.2 and 4.9 ppm, respectively. In contrast to

Table 1 NMR spectral data in ppm for the carbon-carbon double bonds in the DRFs[a]

DRF	^{1}H NMR chemical shifts	^{13}C NMR chemical shifts
1	6.655 (s)	134.8
2	6.625 (s)	134.8
3	6.755 (d, $J = 12.0$ Hz), 6.705 (d, $J = 12.0$ Hz)	135.6, 133.2
4	6.750 (d, $J = 12.0$ Hz), 6.703 (d, $J = 12.0$ Hz)	135.6, 133.2
DiPF	6.810 (s)	130.9

[a]Measured in CDCl3

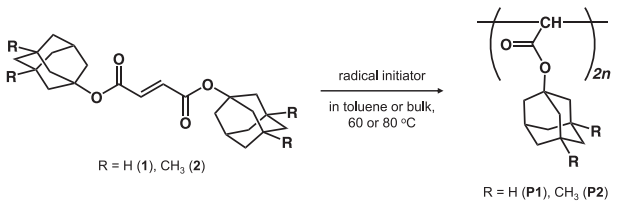

Scheme 3 Conventional radical polymerization of the symmetric DRFs **1** and **2**

Table 2 Radical polymerization of the adamantane-containing DRFs in the presence of a radical initiator either in bulk or in toluene

DRF (g)	Radical initiator (mg)	Solvent (mL)	Temp. (°C)	Time (h)	Yield[a] (%)	M_n[b] $\times 10^{-4}$	M_w/M_n[b]
1 (0.10)	BPO (1.6)	Toluene (0.5)	80	4	0.7	~0.4[c]	[d]
1 (1.00)	BPO (15.6)	Toluene (2.6)	80	24	45.8	0.67	1.35
2 (0.22)	BPO (2.0)	None	80	6	26.0	[e]	[e]
2 (0.22)	MAIB (2.3)	Toluene (0.5)	60	24	9.6	0.37	1.17
3 (0.50)	MAIB (7.8)	None	60	6	54.8	6.38	3.66
3 (0.50)	MAIB (7.9)	Toluene (1.7)	60	24	25.2	0.80	3.62
4 (0.50)	MAIB (7.5)	None	60	4	57.3	6.05	3.82

[a]Based on the weight of the isolated polymer

[b]Determined by SEC

[c]Estimated based on the peak position in the SEC curve

[d]Not determined

[e]Insoluble in THF

the detection of the peaks characteristic of the hydrogen in the side chain, the methine hydrogen of the main chain was hardly observed because of peak broadening. The difficult observation of the peaks attributed to the main chain hydrogen of the PDRFs has often been reported in the literature [2–4]. This suggests the highly restricted motion of the main chain of these adamantane-containing PDRFs.

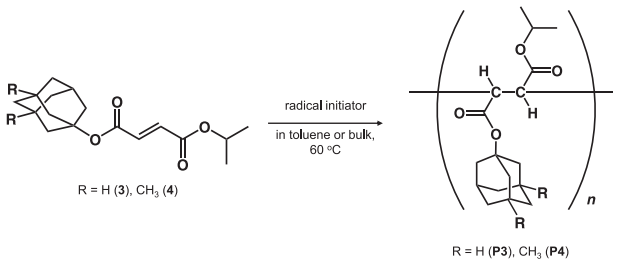

Scheme 4 Conventional radical polymerization of the asymmetric DRFs **3** and **4**

RAFT Polymerization of Adamantane-Containing DRFs

In our previous study [20], it was reported that the polymer chain structures of PDiPF was controlled by the RAFT polymerization using T2 as the bifunctional chain transfer agent (CTA). In this study, therefore, we carried out the RAFT polymerization of the adamantane-containing fumarates using T2. We first investigated the RAFT polymerization behavior of **3** (Scheme 5) in order to synthesize the polymers with functional trithiocarbonate groups at the both chain ends.

When polymerization was carried out with a [**3**]/[T2] molar ratio = 100/1 and at 60 °C for 4–6 h with different MAIB concentrations ([**3**]/[MAIB] molar ratio = 100/2.0–0.35), the corresponding polymer **P3** with a trithiocarbonate moiety located at both chain ends was produced with a 43–50% yield (47–58% conversion). The observed M_n and M_w/M_n values were in the ranges of $1.12–1.33 \times 10^4$ and 2.01, respectively. The M_n and M_w/M_n values decreased to 0.56×10^4 and 1.75, respectively, when the [DRF]/[T2] ratio was changed from 100 to 50. The higher CTA

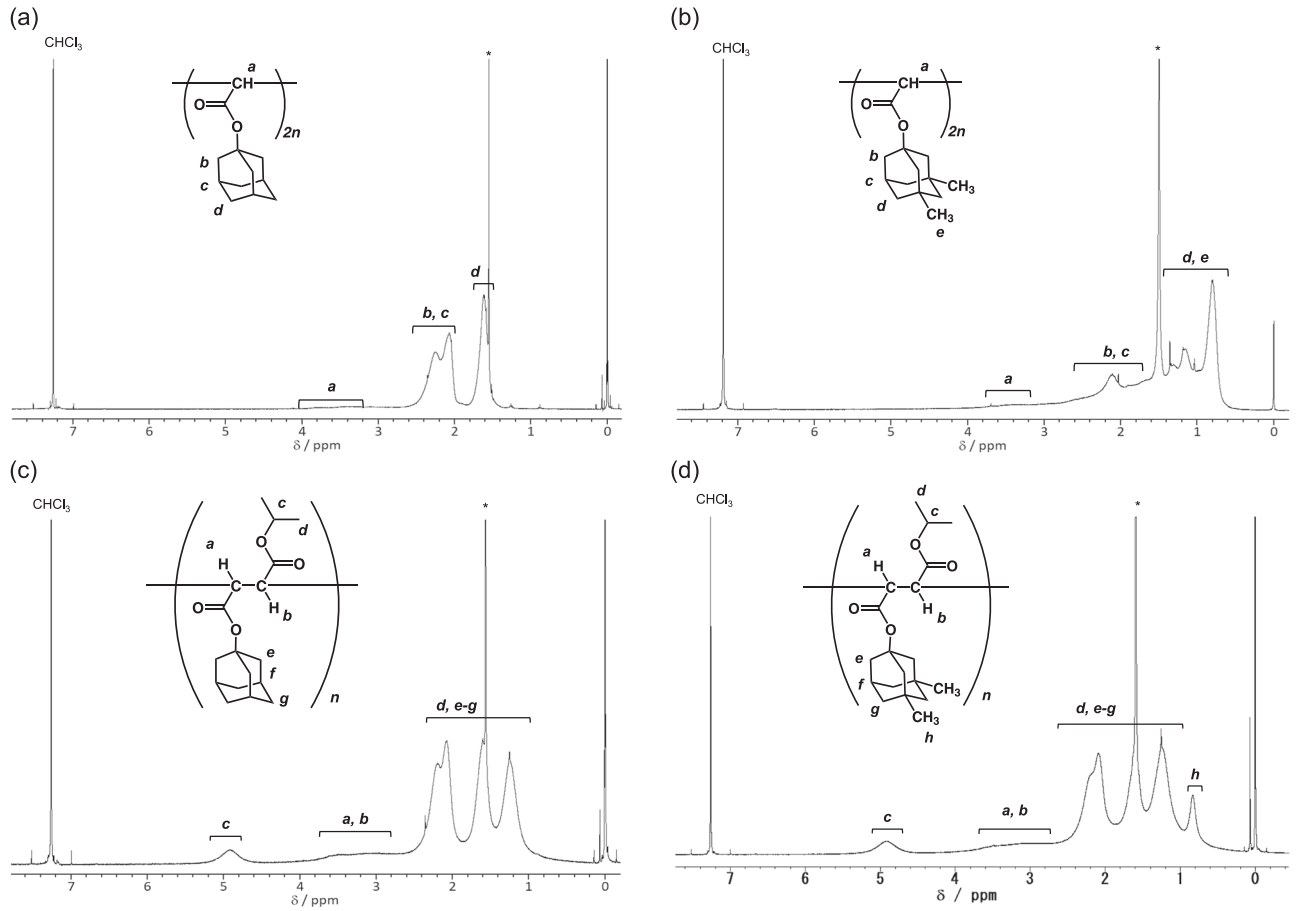

Fig. 5 ^{1}H NMR spectra of **a P1**, **b P2**, **c P3**, and **d P4** in $CDCl_3$

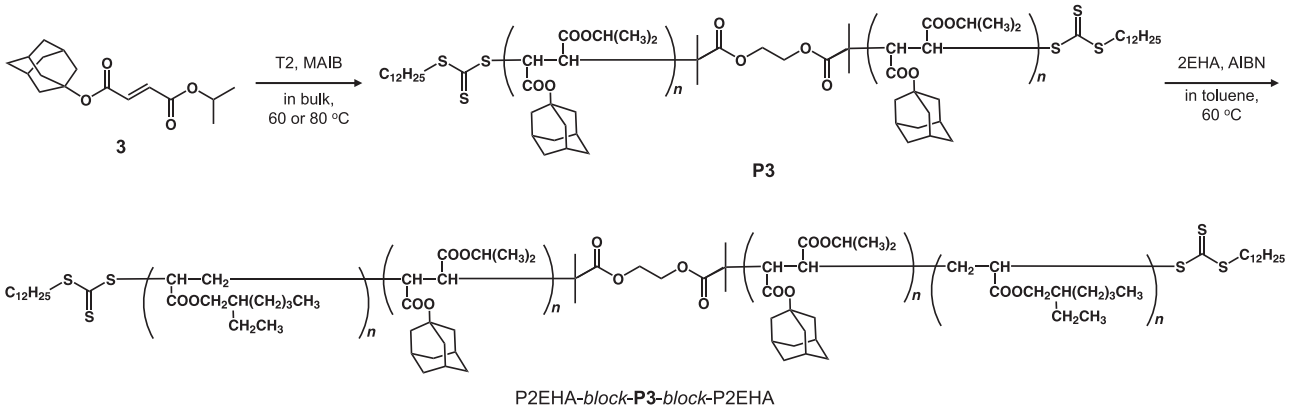

Scheme 5 Synthesis of **P3** and the block copolymer of **P3** with P2EHA (P2EHA-*block*-**P3**-*block*-P2EHA) by RAFT polymerization

Table 3 RAFT polymerization of **3** and **4** in bulk using either T2 or T1F as the CTAs

DRF	CTA	[DRF]/[MAIB]/[CTA] molar ratio	Temp. (°C)	Time (h)	Conv. (%)	Yield (%)	$M_{n,calcd} \times 10^{-4}$	$M_n \times 10^{-4}$	M_w/M_n
3	T2	100/2.0/1.0	60	4.0	47.1	45.3	1.45	1.33	2.01[a]
3	T2	100/0.40/1.0	60	6.0	49.0	49.5	1.51	1.25	2.89[b]
3	T2	100/0.40/1.0	80	4.0	65.0	65.2	1.98	1.34	2.67
3	T2	100/0.35/1.0	60	5.0	58.1	43.0	1.77	1.12	2.16
3	T2	50/0.35/1.0	60	4.0	24.7	17.9	0.44	0.56	1.75
3	T2	50/0.35/1.0	80	2.5	67.2	60.6	1.05	0.87	1.66
3	T1F	200/0.35/1.0	60	4.5	28.2	38.6	1.68	1.59	3.06
3	T1F	100/0.35/1.0	60	5.0	29.1	27.8	0.89	1.67	3.23
DiPF[c]	T2[c]	100/0.35/1.0	80	1.0	52.2	41.0	1.12	1.05	1.28
DiPF	T1F	200/0.35/1.0	80	4.0	78.1	57.6	3.17	4.67	1.27
3/DiPF[d]	T2	100/0.35/1.0	80	4.5	74.8	58.6	1.93	1.51	1.57
4	T2	100/0.40/1.0	60	5.0	30.2	22.0	1.03	0.95	1.64
4	T2	100/0.35/1.0	60	9.0	15.8	14.5	0.58	0.56	1.44

[a]T% and R% were 90% and 93%, respectively. Here, the T% and R% represent the introduction of characteristic fragments at the chain ends and at the center of the resulting PDRFs, respectively (refer to ref. [20]). T: $-SC(=S)S(CH_2)_{11}CH_3$, R: $-C(CH_3)_2COOCH_2CH_2OCOC(CH_3)_2-$

[b]T% and R% were 83% and 86%, respectively

[c]Cited from ref. [20].

[d][**3**]/[DiPF] molar ratio = 1/1 in the feed. The DiPF content in the copolymer was 48.8 mol%

concentration resulted in better control of the reactions, but not enough control was obtained. For the RAFT polymerization of the DRFs, it has been pointed out that the steric hindrance of the leaving group R of the CTAs suppressed the initiation of the DRF polymerization [19], which differs from the RAFT polymerization of conventional monomers, such as methyl methacrylate and styrene. It has been speculated that the larger M_w/M_n values occur due to the slow initiation of the polymerization. We studied the polymerization behavior at a higher temperature (80 °C), but no temperature dependence was observed, as shown in Table 3.

The ^{1}H NMR analysis of the produced polymer chains (Fig. 6(a)) revealed the introduction of the T2 fragment at the polymer chain ends and the R group at the center of the polymer chains with an 83–93% functionality (see the footnotes in Table 3). This indicates that the RAFT polymerization of **3** was capable of controlling the chain-end structure, but control of the molecular weight was still limited. This result was different from the well-controlled polymerization of DiPF using the same CTA and similar polymerization conditions [20]. The isopropyl and adamantyl groups have Taft σ* parameters, which are the polar substituent constants that describe the inductive effects of

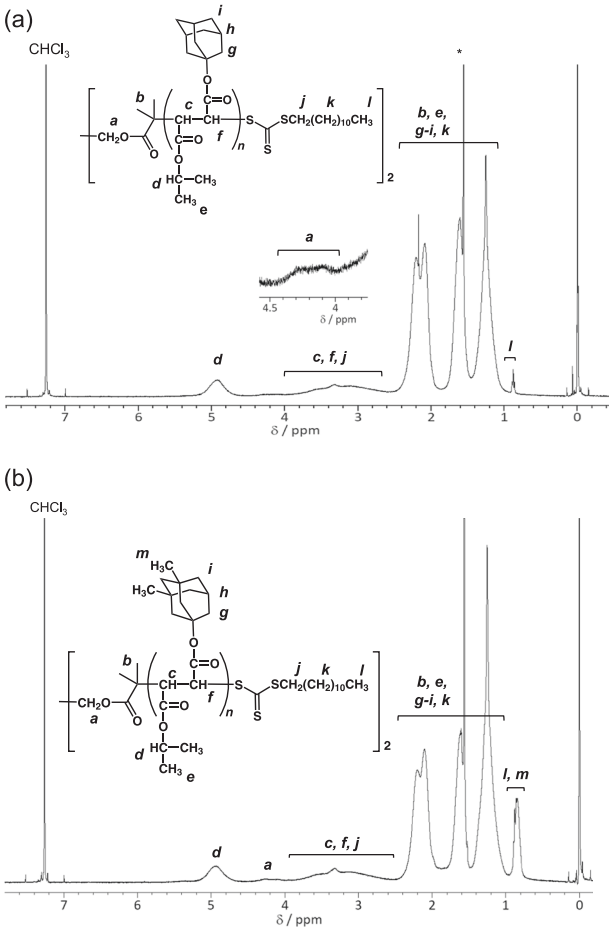

Fig. 6 ^{1}H NMR spectra of **a P3** and **b P4** prepared by RAFT polymerization with T2 at 60 °C

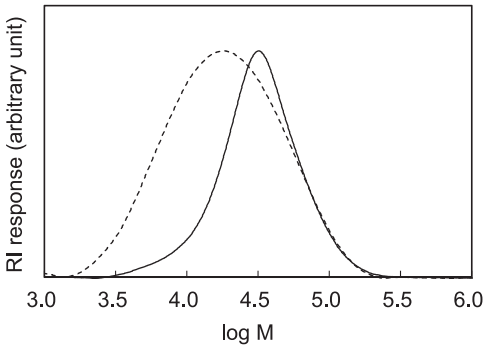

Fig. 7 SEC curves for **P4** (---) and P2EHA-*block*-**P4**-*block*-P2EHA (——) synthesized by RAFT polymerization using T2

the substituents, that are similar to one another, i.e., −0.19 and −0.26, respectively [53]. As shown in Table 3, the polymerization of **4** resulted in smaller M_w/M_n values (1.44–1.64). Unfortunately, the functionality for introducing the CTA fragments into **P4** could not be determined because of the overlap of the characteristic peaks in the ^{1}H NMR spectrum (Fig. 6b). The electron-donating effect of the adamantyl groups was weak but detected by NMR spectroscopy, as shown in Table 1. The ^{1}H NMR chemical shifts of the CH=CH groups changed in the order of 6.810 (for DiPF) > 6.755/6.705 (for **3**) ≥ 6.750/6.703 (for **4**) > 6.655 (for **1**) > 6.625 (for **2**) ppm. In the ^{13}C NMR spectra, the peaks attributed to the C=C carbons were observed at 133.2–135.6 ppm for the adamantane-containing DRFs and 130.9 ppm for DiPF. Introducing an electron-withdrawing group into the ester alkyl group of the primary radical produced from CTA may promote the initiation of the polymerization of the DRFs with electron-donating ester alkyl groups. Actually, we examined this assumption by studying the RAFT polymerization process using the CTA including the electron-withdrawing ester group T1F (Fig. 1). As a result, the degree of control over the living radical polymerization was not improved, even by the introduction of a trifluoromethyl group. These results suggested the importance of the steric hindrance of the adamantyl groups, rather than the polar effect, to the initiation process. We concluded that the steric hindrance of the adamantyl groups obstructed the precise control of the polymerization of the adamantane-containing DRFs. In this study, we decided to further use the produced PDRFs as the macro-CTAs, because the relatively high functionality for the introduction of the trithiocarbonate groups at the chain ends was enough.

Block copolymer synthesis

Block copolymerization was carried out in toluene at 60 °C using 2EHA as the second monomer and **P3** as the macro-CTA ($M_n = 1.25–1.33 \times 10^4$, $M_w/M_n = 2.01–2.89$), which was prepared by the RAFT polymerization of **3** with T2. The copolymer yields were 68–71%, and the M_n increased according to the conversion of 2EHA, as expected. The M_w/M_n values decreased during the polymerization of 2EHA, and finally, copolymers with a narrower molecular weight distribution were isolated ($M_w/M_n = 1.61–1.68$). The block copolymers containing the **P4** segment and the random copolymer segment of **3** and DiPF were synthesized by a similar method. Figure 7 shows the SEC curves for **P4** and P2EHA-*block*-**P4**-*block*-P2EHA, which was synthesized by RAFT polymerization using T2. The peak in the SEC curve shifted to the high molecular weight region after the block copolymerization. In Fig. 8, the ^{1}H NMR spectra of the resulting block copolymers are shown. Based on the peak intensity ratio of the characteristic peaks in the spectra, we calculated the DRF contents in the copolymers, which were compared with those determined from the change in the M_n values for the macro-CTA and the resulting block copolymer. As shown in Table 4, both the DRF content values agreed with each other.

Next, the thermal properties of the PDRFs and their block copolymers combined with polyacrylates were investigated by TG analysis. The TG curves of the selected PDRFs are shown in Fig. 9. The determined T_{d5} and T_{max} values are summarized in Table 5. The onset temperature for the decomposition of the DRFs increased by the introduction of adamantyl ester groups, while the decomposition of DiPF started below 250 °C. The T_{d5} and T_{max} values for **P1** and **P2** were much higher than those of PDiPF. The **P3** and **P4** compounds containing both the adamantyl and isopropyl ester groups had moderate thermal stabilities (T_{d5} = 286–288 °C). The triblock copolymers of the adamantane-containing PDRF with P2EHA also exhibited high decomposition temperatures. An excellent thermal stability was already reported for the polymers containing AdA repeating units [48, 49].

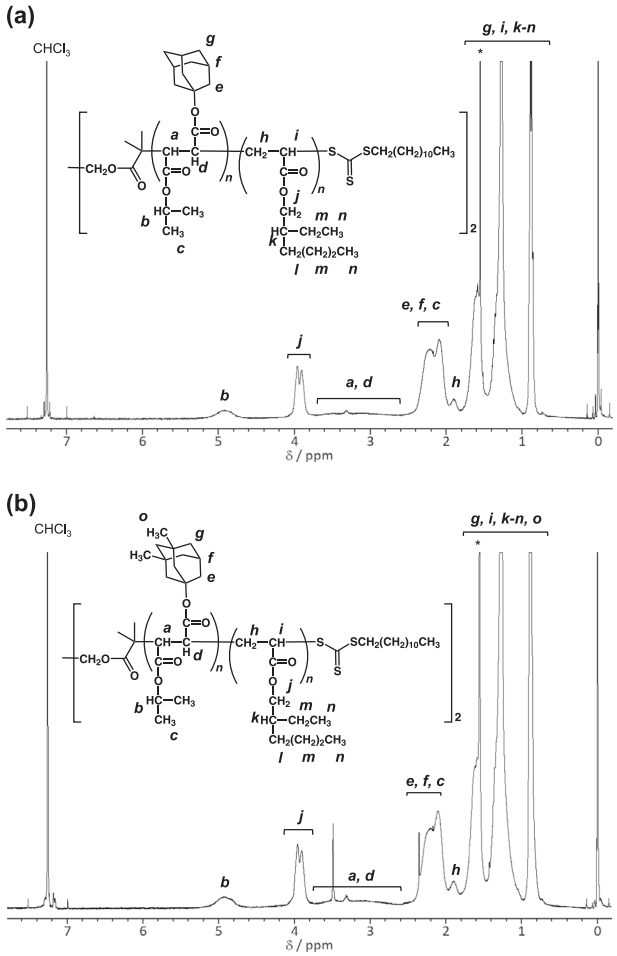

Fig. 8 ^{1}H NMR spectra of **a** P2EHA-*block*-**P3**-*block*-P2EHA and **b**

The triblock copolymers containing the rigid poly(substituted methylene)s and the soft P2EHA segments were soluble or swelled in many types of organic solvents, including hexane, cyclohexane, ethyl acetate, and methyl ethyl ketone (refer to Table S1 in the Supporting Information). Some of the corresponding PDRF homopolymers were insoluble in hexane, ethyl acetate, methyl ethyl ketone, and acetone. The introduction of asymmetric structures to the adamantane-containing DRF monomers improved the solubility of not only the DRF monomers but also the corresponding PDRFs. The triblock copolymer of **P4** with P2EHA exhibited the best solubility.

The optical properties of the polymers were also investigated. The homopolymers **P1–P4** were too brittle to prepare a cast film to evaluate their optical properties. In contrast, a highly transparent thin film was successfully prepared from the block copolymer of **P3** with P2EHA by casting and was similar to the PDiPF and PAdA films previously reported in the literature [20, 48]. The results are shown in Fig. 10 and Table 6. The transmittance of visible light at 400 nm was higher than 90% for P2EHA-*block*-**P3**-*block*-P2EHA. The microphase separated structure of the copolymers may form in the block copolymers [48], which had no significant effect on the light scattering, because the

Table 4 Block polymerization of 2EHA using the PDRFs as the macro-CTA in toluene at 60 °C[a]

Macro-CTA ($M_n \times 10^{-4}$, M_w/M_n)	[2EHA]/[AIBN]/[CTA] molar ratio	Time (h)	Conv. (%)	Yield (%)	$M_{n,calcd} \times 10^{-4}$	$M_n b \times 10^{-4}$	M_w/M_n[b]	DRF mol%	
								NMR	SEC
P3 (1.33, 2.01)	100/0.2/1	4	72.1	70.5	2.66	2.47	1.61	40	41
P3 (1.25, 2.89)	100/0.2/1	4	56.3	68.3	2.28	2.67	1.68	41	34
P4 (0.95, 1.64)	50/0.2/1	3	75.9	70.0	1.65	1.87	1.32	46	35
P(**3**/DiPF)[c]	100(MA)/0.28/1	4	79.2	79.1	2.19	2.33	1.38	52	38
PDiPF (1.05, 1.28)	200/0.20/1	3	62.6	57	3.37	3.44	1.34	31	27
PDiPF (1.05, 1.28)	200/0.20/1	10	83.8	73.0	4.11	3.81	1.41	28	22

MA methyl acrylate

[a]2EHA(or MA)/toluene = 1/1 by weight

[b]Determined by SEC

[c]Random copolymer of **3** and DiPF with $M_n = 1.51 \times 10^4$, $M_w/M_n = 1.57$, DiPF 48.8 mol%
P2EHA-*block*-**P4**-*block*-P2EHA in $CDCl_3$

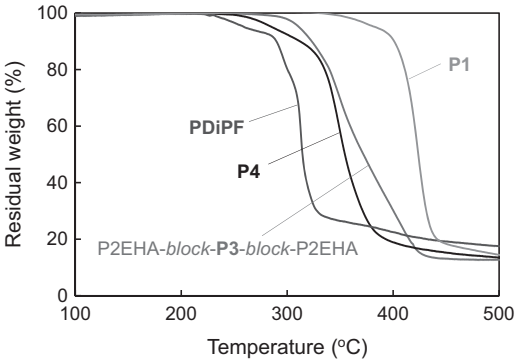

Fig. 9 TG curves of **P1**, **P4**, P2EHA-*block*-**P3**-*block*-P2EHA, and PDiPF measured under a nitrogen stream at a heating rate of 10 °C/min

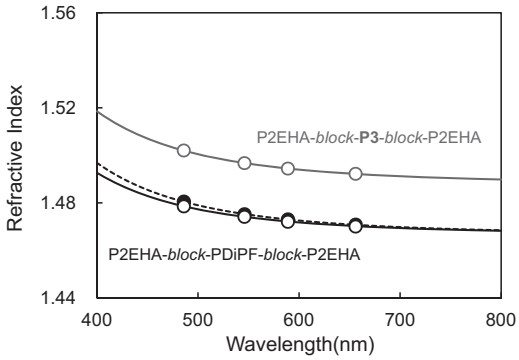

Fig. 10 Wavelength dependence of the refractive indices of P2EHA-*block*-**P3**-*block*-P2EHA (red) and P2EHA-*block*-PDiPF-*block*-P2EHA before (blue, solid curve) and after (blue, dotted curve) reduction to remove the RAFT groups at the polymer chain ends

Table 5 Thermal decomposition temperatures of adamantane-containing PDRFs and the triblock copolymers with P2EHA[a]

Polymer	T_{d5} (°C)	T_{max} (°C)
P1	384	425
P2	329	397
P3	288	348
P4	286	350
P(**3**/DiPF)	281	293
PDiPF	259	296, 314
P2EHA-*block*-**P3**-*block*-P2EHA	311	350, 319
P2EHA-*block*-**P4**-*block*-P2EHA	317	344, 397
PMA-*block*-P(**3**/DiPF)-*block*-PMA	296	330
PMA	322	404
PAdA[b]	358	–
PAdA-*block*-PnBA[b,c]	343	–

PMA poly(methyl acrylate)

[a]Determined by TG under a nitrogen stream at a heating rate of 10 °C /min

[b]Cited from ref. [48]

[c]Diblock copolymer of PAdA and poly(*n*-butyl acrylate) (PnBA) with an AdA content of 52.5 mol%

domain size was smaller than the wavelength of the light. The n_D value of P2EHA-*block*-**P3**-*block*-P2EHA (1.494) was similar to the n_D values of the other adamantane-containing polyacrylates, such as PAdA and its block copolymer [48], and conventional polymethacrylates, including poly(methyl methacrylate) ($n_D = 1.49–1.51$) [54], and slightly higher than the n_D values of the polymers including the PDiPF segment ($n_D = 1.463–1.473$), as shown in Table 6. A previous study [20] demonstrated that the transmittance of the block copolymers synthesized by the RAFT polymerization increased after the reduction of the RAFT moiety at the polymer chain end, and simultaneously, the n_D values slightly decreased because of the presence of trithiocarbonate groups with C=S bonds that are highly polarizable. These results indicated that the trithiocarbonate groups surely influenced the optical properties, such as the refractive indices at a short wavelength and the Abbe number, but this effect was much smaller compared with the effect of introducing the adamantyl moiety in the side chain.

PDRFs are one of least flexible polymers. For example, the Kuhn's statistical segment length, which corresponds to twice the persistence length, was determined to be 22 nm for PDiPF based on the dilute solution properties [14–16]. It has also been verified that the rigidity of the PDRF chains is sensitive to the bulkiness of the ester alkyl groups in the side chain [17]. Figure 11 shows the X-ray diffraction profiles of various PDRFs and triblock copolymers including PDRF segments. In Table 7, the *d* values calculated from the position of the diffraction peak are summarized together with the diameter of the polymer chains, which were estimated based on the molecular models. All the PDRFs and their block copolymers had strong peaks located in the low angle region of $q =$ 4–6 nm^{-1} and amorphous halos in the wide angle range of $q = 10–15\ nm^{-1}$. The *d* values increased with an increase in the bulkiness of the ester alkyl groups of the DRF repeating unit in the following order: isopropyl < adamantyl <3,5-dimethyl-1-adamantyl. The **P3** with an asymmetric repeating structure exhibited an intermediate *d* value between those of PDiPF and **P2**. These characteristic peaks at low angles are due to the rigid PDRF segments. Diffraction in the low angle region was not observed for the vinyl polymers containing the adamantyl groups, such as PAdA. It should be noted that these *d* values agree with the diameters of the PDRF chains. The rigid PDRF chains possibly assembled to form any aggregates present in the solid-state.

Table 6 Optical properties of the PDRFs and polyacrylates and their block copolymers

Polymer	DRF content (mol%)	Transmittance at 400 nm (%)	n_D (589 nm)	ν_D
P2EHA-*block*-**P3**-*block*-P2EHA	59	90.2	1.4944	50.5
P2EHA-*block*-PDiPF-*block*-P2EHA[a]	83	88.5 (90.6)[b]	1.4730 (1.4724)[b]	48.9 (55.5)[b]
PDiPF[c]	100	90.6	1.4634	57.2
PAdA[d]	0	92.8	1.4913	45.3
PAdA-*block*-PnBA[d,e]	0	92.8 (at 380 nm)	1.4915	46.5

[a]Cited from ref. [20]

[b]Values in parentheses indicate the value obtained after reduction to remove the RAFT groups at the polymer chain ends

[c]Prepared by conventional radical polymerization

[d]Cited from ref. [48]

[e]Diblock copolymer of PAdA and poly(*n*-butyl acrylate) (PnBA) with an AdA content of 52.5 mol%

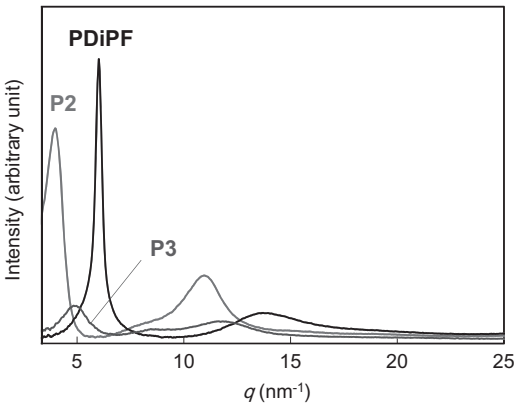

Fig. 11 X-ray diffraction profiles obtained for **P2**, **P3**, and PDiPF

Table 7 X-ray diffraction data for the PDRFs and their block copolymers

Polymer	q (nm^{-1})	d value (Å)	Diameter[a] (Å)
P2	4.00	15.7	14.5
P3	4.86	12.9	12.1
PDiPF	6.02	10.4	10.3
P2EHA-*block*-**P4**-*block*-P2EHA	4.79	13.1	12.1
P2EHA-*block*-PDiPF-*block*-P2EHA	6.02	10.4	10.3

[a]Diameter of the polymer chain estimated using the molecular model

Conclusion

In this study, we synthesized four kinds of DRFs containing adamantyl groups and used them to carry out conventional radical polymerization and RAFT polymerization. It has been demonstrated that the introduction of methyl substituents into the adamantyl moiety and an asymmetric ester structure into the fumarates lowered the melting points and changed the solubility of the adamantane-containing fumarate monomers. Block copolymers consisting of a rigid PDRF segment and a flexible polyacrylate segment were prepared by RAFT polymerization. It was confirmed that the adamantane-containing PDRFs and their block copolymers with a polyacrylate were thermally stable. The X-ray diffraction experiments revealed that the adamantane-containing PDRF chains aggregated in the solid-state. We are now continuing to study the aggregation and chain dynamics of the DRFs with different chain rigidities.

Acknowledgements The synchrotron radiation experiments were performed at the BL40B2 of the SPring-8 beamline with the approval of the Japan Synchrotron Radiation Research Institute (JASRI) (Proposals No. 2018B1141). We acknowledge the experimental support of Dr. Noboru Ohta and Dr. Hiroshi Sekiguchi at SPring-8.

Compliance with ethical standards

Conflict of interest The authors declare that they have no conflict of interest.

References

1. Otsu T, Ito O, Toyoda N, Mori S. Polymers from 1,2-disubstituted ethylenic monomers. 2. Homopolymers from dialkyl fumarates by radical initiator. Makromol Chem Rapid Commun. 1981;2:725–8.
2. Otsu T, Yasuhara T, Shiraishi K, Mori S. Radical high polymerization of di-*tert*-butyl fumarate and novel synthesis of high molecular weight poly(fumaric acid) from its polymer. Polym Bull. 1984;12:449–56.
3. Otsu T, Yasuhara T, Matsumoto A. Synthesis, characterization, and application of poly(substituted methylene)s. J Macromol Sci-Chem. 1988;A25:537–54.

4. Matsumoto A, Otsu T. Detailed mechanism of radical high polymerization of sterically hindered dialkyl fumarates. Macromol Symp. 1995;98:139–52.
5. Kitano T, Fujimoto T, Nagasawa M. Preparation and characterization of a monodisperse, semiflexible polymer, poly(*tert*-butyl crotonate). Macromolecules. 1974;7:719–23.
6. Matsumoto A, Horie A, Otsu T. Synthesis and characterization of thermally stable polymers through anionic polymerization of *tert*-alkyl crotonates. Polym J. 1991;23:211–8.
7. Ihara E, Haida N, Iio M, Inoue K. Palladium-mediated polymerization of alkyl diazoacetates to afford poly(alkoxycarbonylmethylene)s. First synthesis of polymethylenes bearing polar substituents. Macromolecules. 2003;36:36–41.
8. Shikinaka K, Suzuki K, Masunaga H, Ihara E, Shigehara K. Stiff- & hierarchical-chain nature of atactic and stereoregular poly (substituted methylene)s. Polym Int. 2018;67:495–9.
9. Yamada K, Takayanagi M, Murata Y. Relations between molecular aggregation state and mechanical properties in poly(diisopropyl fumarate). Polymer. 1986;27:1054–7.
10. Choi SB, Takahara A, Amaya N, Murata Y, Kajiyama T. Effects of ester side chain structure on gas permeation behavior of poly (dialkyl fumarate)s. Polym J. 1989;21:433–8.
11. Park K, Kikuchi H, Kajiyama T. Component dependence of aggregation structure and light scattering properties of polymer/liquid crystal composite films. Polym J. 1994;26:895–904.
12. Jeong HK, Kikuchi H, Kajiyama T. Low voltage light switching of hybrid-type cell composed of (polymer/liquid crystal) composite system. Polym J. 1997;29:165–70.
13. Matsumoto A, Tarui T, Otsu T. Dilute solution properties of semiflexible poly(substituted methylenes): intrinsic viscosity of poly(diisopropyl fumarate) in benzene. Macromolecules. 1990;23:5102–5.
14. Matsumoto A, Nakagawa E. Evaluation of chain rigidity of poly (diisopropyl fumarate) from light scattering and viscosity in tetrahydrofuran. Eur Polym J. 1999;35:2107–13.
15. Nakatsuji M, Hyakutake M, Osa M, Yoshizaki T. Mean-square radius of gyration and second virial coefficient of poly(diisopropyl fumarate) in dilute solution. Polym J. 2008;40:566–71.
16. Nakatsuji M, Soutoku K, Osa M, Yoshizaki T. Transport coefficients of poly(diisopropyl fumarate) in dlute solution. Polym J. 2009;41:83–89.
17. Awazu N, Komatsubara T, Osa M, Yoshizaki T. Dilute solution properties of poly(di-*tert*-butyl fumarate). Polym J. 2016;48:991–7.
18. Matsumoto A, Maeo N, Sato E. Living radical polymerization of diisopropyl fumarate to obtain block copolymers containing rigid poly(substituted methylene) and flexible polyacrylate segments. J Polym Sci, Part A: Polym Chem. 2016;54:2136–47.
19. Takada K, Matsumoto A. Reversible addition-fragmentation chain transfer polymerization of diisopropyl fumarate using various dithiobenzoates as chain transfer agents. J Polym Sci, Part A: Polym Chem. 2017;55:3266–75.
20. Takada K, Matsumoto A. Synthesis of transparent block copolymers consisting of poly(diisopropyl fumarate) and poly(2-ethylhexyl acrylate) segments by reversible addition-fragmentation chain transfer polymerization using trithiocarbonates as the chain transfer agents. J Polym Sci, Part A: Polym Chem. 2018;56:2584–94.
21. Fort RC Jr., Schleyer PvR. Adamantane: consequences of the diamondoid structure. Chem Rev. 1964;64:277–300.
22. Chern Y, Chung W. Preparation and properties of polyamides and polyimides drived from 1,3-diaminoadamantane. J Polym Sci, Part A: Polym Chem. 1996;34:117–24.
23. Hsiao S-H, Li C-T. Synthesis and characterization of new adamantane-based polyimides. Macromolecules. 1998;31:7213–7.
24. Seino H, Mochizuki A, Ueda M. Synthesis of aliphatic polyimides containing adamantyl units. J Polym Sci, Part A: Polym Chem. 1999;37:3584–90.
25. Acar HY, Jensen JJ, Thigpen K, McGowen JA, Mathias LJ. Evaluation of the spacer effect on adamantane-containing vinyl polymer Tg's. Macromolecules. 2000;33:3855–9.
26. Liaw D-J, Liam B-Y. Synthesis and characterization of new polyamide-imides containing pendent adamantyl groups. Polymer. 2001;42:839–45.
27. Kameshima H, Nemoto N, Sanda F, Endo T. Cationic ring-opening polymerization of five-membered cyclic thiocarbonate bearing and adamantane moiety via selective ring-opening direction. Macromolecules. 2002;35:5769–73.
28. Fukukawa K, Shibasaki Y, Ueda M. A photosensitive semi-alicyclic poly(benzoxazole) with high transparency and low dielectric constant. Macromolecules. 2004;37:8256–61.
29. Hashimoto T, Makino Y, Urushisaki M, Sakaguci T. Living cationic polymerization of 2-adamantyl vinyl ether. J Polym Sci, Part A: Polym Chem. 2008;46:1629–37.
30. Cho YS, Allcock HR. Synthesis of adamantyl polyphosphazene–polystyrene block copolymers, and β-cyclodextrin-adamantyl side group complexation. Macromolecules. 2009;42:4484–90.
31. Ando S, Koyama Y, Miyata S, Sato S, Kanehashi S, Nagai K. Synthesis and characterization of ABA-type triblock copolymers derived from polyimide and poly(2-methyl-2-adamantyl methacrylate). Polym Int. 2014;63:1634–42.
32. Lu W, Huang C-L, Hong K-L, Kang N-G, Mays JW. Poly(1-adamantyl acrylate): Living anionic polymerization, block copolymerization, and thermal properties. Macromolecules. 2016;49:9405–14.
33. Lu W, Yin P, Osa M, Wang W, Kang N, Hong K, et al. Solution properties, unperturbed dimensions, and chain flexibility of poly (1-adamantyl acrylate). J Polym Sci, Part B: Polym Phys. 2017;55:1526–31.
34. Otsu T, Matsumoto A, Horie A, Tanaka S. Synthesis of thermally stable vinyl polymers from adamantyl-containing acrylic derivatives. Chem Lett. 1991;20:1145–8.
35. Matsumoto A, Tanaka S, Otsu T. Synthesis and characterization of poly(1-adamantyl methacrylate): effects of the adamantyl group on radical polymerization kinetics and thermal properties of the polymer. Macromolecules. 1991;24:4017–24.
36. Matsumoto A, Tanaka S, Otsu T. Local conformation of poly(1-adamantyl methacrylate) evaluated from intrinsic viscosity. Colloid Polym Sci. 1992;270:17–21.
37. Matsumoto A, Watanabe H, Otsu T. Synthesis and radical polymerization of itaconates containing an adamantyl ester group. Bull Chem Soc Jpn. 1992;65:846–52.
38. Matsumoto A, Otsu T. Synthesis and radical polymerization of adamantyl-containing maleic and fumaric esters leading to formation of thermally stable poly(substituted methylene)s with a rigid chain structure. Chem Lett. 1991;20:1361–4.
39. Matsumoto A, Horie A, Otsu T. Synthesis and thermal properties of poly(adamantyl sorbate). Makromol Chem Rapid Commun. 1991;12:681–5.
40. Ishizone T, Tajima H, Torimae H, Nakahama S. Anionic polymerization of 1-adamantyl methacrylate and 3-methacryloyloxy-1,1′-biadamantane. Macromol Chem Phys. 2002;203:2375–84.
41. Kobayashi S, Matsuzawa T, Matsuoka S, Tajima H, Ishizone T. Living anionic polymerizations of 4-(1-adamantyl)styrene and 3-(4-vinylphenyl)-1,1′-biadamantane. Macromolecules. 2006;39:5979–86.
42. Kobayashi S, Kataoka H, Ishizone T, Kato T, Ono T, Kobutaka S, et al. Synthesis and properties of new thermoplastic elastomers containing poly[4-(1-adamantyl)styrene] hard segments. Macromolecules. 2008;41:5502–8.

43. Kobayashi S, Kataoka H, Ishizone T. Synthesis of well-defined poly(ethylene-alt-1-vinyladamantane) via living anionic polymerization of 2-(1-adamantyl)-1,3-butadiene, followed by hydrogenation. Macromolecules. 2009;42:5017–26.
44. Kobayashi S, Kataoka H, Ishizone T, Kato T, Ono T, Kubotaka S, et al. Synthesis of well-defined random and block copolymers of 2-(1-adamantyl)-1,3-butadiene with isoprene via anionic polymerization. React Funct Polym. 2009;69:409–15.
45. Kang B-G, Shoji H, Kataoka H, Kurashima R, Lee J-S, Ishizone T. Living anionic polymerization of N-(1-adamantyl)-N-4-vinylbenzylideneamine and N-(2-adamantyl)-N-4-vinylbenzylideneamine: effect of adamantyl groups on polymerization behaviors and thermal properties. Macromolecules. 2015;48:8489–96.
46. Matsuoka D, Goseki R, Uchida S, Ishizone T. Living anionic polymerization of 1-adamantyl 4-vinyl phenyl ketone. Macromol Chem Phys. 2017;218:1700015.
47. Kobayashi S, Kataoka H, Goseki R, Ishizone T. Living anionic polymerization of 4-(1-adamantyl)-α-methylstyrene. Macromol Chem Phys. 2018;219:1700450.
48. Nakano Y, Sato E, Matsumoto A. Synthesis and thermal, optical, and mechanical properties of sequence-controlled poly(1-adamantyl acrylate)-block-poly(*n*-butyl acrylate) containing polar side group. J Polym Sci, Part A: Polym Chem. 2014;52:2899–910.
49. Matsumoto A, Sumihara T. Thermal and mechanical properties of random copolymers of diisopropyl fumarate with 1-adamantyl and bornyl acrylates with high glass transition temperatures. J Polym Sci, Part A: Polym Chem. 2017;55:288–96.
50. Suzuki Y, Tsujimura T, Funamoto K, Matsumoto A. Relaxation behavior of random copolymers containing rigid fumarate and flexible acrylate segments by dynamic mechanical analysis. Polym J. 2019. https://www.nature.com/articles/s41428-019-0226-z
51. Zhang C, Kim DS, Lawrence J, Hawker CJ, Whitaker AK. Elucidating the impact of molecular structure on the ^{19}F NMR dynamics and mri performance of fluorinated oligomers. ACS Macro Lett. 2018;7:921–6.
52. Jenkins FA, White HF. Fundamentals of optics. 4th ed. McGraw-Hill: New York; 1976. p. 479.
53. Hansch C, Leo LJ. Substituent constants for correlation analysis in chemistry and biology. John Wiley & Sons: New York; 1979.
54. Ozaki A, Sumita K, Goto K, Matsumoto A. Synthesis of poly(decahydro-2-naphthyl methacrylate)s with different geometric structures and effects of side-group dynamics on polymer properties investigated by thermal and dynamic mechanical analyses and DFT calculations. Macromolecules. 2013;46:2941–50.